International Journal of Robotics and Control Systems
Vol. 5, No. 2, 2025, pp. 862-880
ISSN 2775-2658
http://pubs2.ascee.org/index.php/ijrcs

Cross-Age Face Verification Using Generative Adversarial Networks (GAN) with Landmark Feature

Fahmi Syuhada [a,1,*], Yuan Sa'adati [a,2]

[a] Department of Computer Science, University of Qamarul Huda Badaruddin Bagu, Nusa Tenggara Barat, Central Lombok 83511, Indonesia
[1] fahmisy@uniqhba.ac.id; [2] yuan@uniqhba.ac.id
* Corresponding Author

ARTICLE INFO

Article history
Received December 30, 2024
Revised February 09, 2025
Accepted March 06, 2025

Keywords
Cross-Age;
Face-Verification;
GAN;
Landmark;
Synthesis

ABSTRACT

Cross-age face verification is a complex problem in biometric recognition in terms of aging, a naturally changing face structure, and face landmark configuration changes over time. In this paper, a new cross-age face verification method is proposed with a Generative Adversarial Network (GAN) and a mix of landmark-based features. Realistic aging of a face with identity-specific landmarks, such as eyes, nose, and mouth, is generated for effective face recognition in a range of age groups. Performance testing with an in-house collected face dataset of 200 face images exhibited effectiveness in changing face configuration and face shape transformations, such as a fuller face thinning and thin face becoming fuller. Comparison with direct face verification showed increased values of similarity, such as 32.57% to 63.80%, reduced values of feature distance, such as 0.6743 to 0.3620, and improvement in accuracy for the ArcFace, VGG-Face, and Facenet architectures. ArcFace exhibited an improvement in accuracy with an increase in value from 82.64% to 86.02%, VGG-Face with an improvement in value from 76.23% to 80.57%, and Facenet with an improvement in value from 67.54% to 74.48%. These observations validate the effectiveness of the proposed method in overcoming age-related complications and improving cross-age face verification performance. In future work, we plan to investigate a larger dataset and model refinement to realize performance improvement and real-life biometric suitability.

1. Introduction

Face recognition technology allows the verification of identity based on unique facial features. [1]-[5]. This technology uses algorithms and software to collect, analyze, and compare facial features stored in a database, and then determines the similarity level between two faces. By identifying facial characteristics such as the distance between the eyes, the shape of the nose, or the contours of the face, this technology can provide accurate results in the process of face recognition or matching [6]-[8]. Applications of this technology can be found in various fields, including security, biometric authentication, and forensic investigations, as well as in the development of more advanced AI-based systems [9]. Currently, the population census data has implemented identity verification for individuals based on their identity card data. This is useful for ensuring the validity of identity data based on facial verification that has been stored during registration.

While this technology has achieved remarkable accuracy in various applications, its performance deteriorates significantly when verifying faces across different age periods. This challenge, known as cross-age face verification, arises because of natural facial aging and changes in physical landmarks over time [10], [11]. These changes pose critical issues for applications like identity verification systems that rely on historical facial data, such as identity card photos that are often taken decades apart [12]. This paper focuses on addressing the cross-age face verification problem, where significant differences in facial features over time hinder accurate identification. The inability of existing models to adapt to both age-related changes and landmark transformations often results in suboptimal verification performance [13], [14].

Face verification studies have identified factors that affect the sensitivity evaluation outcomes of the verification process [15]-[17]. The issue is whether the current face can be verified if the data used were registered long ago or during youth. This issue occurs frequently in identity card photo verification. Typically, individuals register when they are young. Since identity cards are valid for life, they do not update their facial data [18], [19]. Facial changes are bound to occur over time. The challenge is to determine how a model can verify the face in such cases.

Cross-age face verification is an intriguing research challenge. Ramanathan and Chellappa [20] conducted a study on age-based facial development by modeling Bayesian classification. Subsequently, cross-age face verification was performed using a discriminative approach. A critical aspect of this study is the facial feature vector, which comprises gradient orientation parameters [21]. Other research has developed models such as the Hierarchical Local Binary Pattern, a set of linear equations for craniofacial growth parameters, the Bacteria Foraging Fusion Algorithm, the Alternating Greedy Coordinate Descent Algorithm, and the K-means Algorithm with features including eyes, nose, chin, ears, and lips [22]-[26].

Although quite a few prior studies reported significant achievements in cross-age face verification, most of them did not consider the crucial limitations of conventional approaches. Most traditional approaches rely on a type of Bayesian classification model or an approach based on handcrafted features, which fail to adapt well to complex variations due to aging and changes in facial landmarks. For example, features based on gradient orientation [20] and hierarchical local binary patterns [21] are quite successful in the representation of texture; however, they are weakly capable of modeling nonlinear facial aging over decades. In the same vein, methods that rely on a craniofacial growth model [22] rely heavily on predefined growth parameters and thus can hardly generalize to different populations.

Direct approaches based on facial image synthesis represent a state-of-the-art cross-age verification method [27], [28]. Test facial images are synthesized to reflect specific ages, resulting in the creation of new faces [29], [30]. Subsequently, verification can be conducted within the same age group. Duong et al. [31] developed a generative probabilistic model to simulate the process of facial aging. Generative Adversarial Networks (GANs) synthesize facial images to create new faces. GANs are an unsupervised learning technique in deep learning that automatically learns patterns from the input facial data and is then used to synthesize new facial images.

To facilitate GAN training, a previous study [32] proposed the Deep Convolutional GAN framework, which has promoted the application of GANs in various tasks, such as video prediction and cross-domain image generation [33], [34]. Arjovsky et al. [35] performed a rigorous analysis of the GAN objective and its instability during the training phase, which led to the development of Wasserstein GANs. Shortly after WGAN, an improved version of WGAN was proposed. The study [36] modeled Conditional GANs, which use prior information in image generation. Reed et al. demonstrated the ability to generate realistic images from text descriptions [37]. CycleGAN was also successfully applied to image-to-image translation tasks, achieving good performance. The proposed method significantly improves the performance of GANs in image generation [38]. Wang et al. designed the Identity-Preserved Conditional Generative Adversarial Networks (IPCGANs) framework. The Conditional Generative Adversarial Networks module functions as a realistic face synthesis that aligns with the target. The Identity-Preserved module retains identity information, and the age classifier enforces the generated face to match the target age [39]. Despite these advances, current GAN-based methods focus primarily on age progression or regression without specifically addressing transformations in facial landmarks induced by aging, such as changes in facial fullness or shifts in the structure of jawlines and cheekbones.

The specific problem proposed in this paper is that past facial data or historical facial images may exhibit different characteristics than contemporary facial images. For example, there may be differences in facial landmarks; for example, older faces have chubby landmarks, whereas current faces are slim, and vice versa. Research into facial development, particularly GAN methods, that addresses this issue has not yet been conducted. This condition affects the verification results if facial aging is performed without considering the current facial conditions. In this paper, we propose a GAN model to verify cross-age faces by combining the landmark characteristics of past and current faces. The proposed GAN was developed not only to perform aging based on age and to consider the differences in landmark changes between the two faces being verified. The proposed initial methodology is divided into several processes. These include determining and capturing age and landmark data from the current facial image. Then, a test face image is developed based on the obtained features. Finally, verification was conducted between the current face and the synthesized test face image.

2. Method

This section provides a comprehensive explanation of the research methods employed in the proposed design for Cross-Age Face Verification. Fig. 1 illustrates the step-by-step progression of the process. The process starts with Data Collection, Cross-Age Face Synthesis, Landmark Detection, Face-Landmark Synthesis, and concludes with the Verification Process.

2.1. Data Collection

At this stage, the processing of the required data for this study is initiated. The acquisition and preprocessing of the data required for this study are initiated at this stage. The dataset used in this study comprises cross-age facial images that were curated to facilitate an in-depth analysis of age-related variations. The data requirements are identified to determine the types of data used, considering crucial factors such as age progression, ethnicity, facial expressions, lighting conditions, and camera angles to ensure a diverse and representative dataset.

The dataset used in this study comprised face photos acquired through various sources, public databases, social networks, and explicit searches through search engines, such as Google. The dataset was compiled with care in a manner such that each individual had a minimum of two photos: a past-face and a current-face, with a well-established age interval between them. The used dataset effectively portrays significant variations in face structures over a period, particularly face landmark configuration changes, allowing for a thorough analysis of cross-age face verification.

To enhance the usability and quality of the dataset, preprocessing for face alignment, face normalization, and facial landmark detection was conducted. The preprocessing phase played a significant role in minimizing variations in factors not age-related, including the head pose and variations in illuminating conditions. In addition, filtering out low-quality face images helped preserve the sharpness and uniformity of face landmark positioning in the dataset. The proposed dataset constitutes a basis for testing the proposed cross-age face verification scheme for robustness and accuracy and provides useful information about the impact of age-related face transformations on face recognition performance.

2.2. Cross-Age Face Synthesis

The next stage of the proposed method, referred to as Cross-Age Face Synthesis, harmonizes the perceived age between a past face and current face representations. The direct approaches involving facial image synthesis are methods for cross-age verification. Past face images are synthesized to align with current face ages, effectively generating new face representations at the desired age stages.

Subsequently, verification was performed within the same age group, ensuring more accurate comparisons [31]. The Generative Adversarial Network (GAN) is a method developed to perform facial aging, enabling the synthesis of realistic age-progressed or age-regressed face images while maintaining the individual's identity [39]-[43]. Generative adversarial networks (GANs) consist of two main components: the Generator and the Discriminator. GANs operate based on a competitive principle, where the Generator produces synthetic images, and the Discriminator evaluates these images by comparing them with real images [44]. The fundamental equation of GANs is a minimax problem between the generator and discriminator, which is expressed as follows:

$$\min_{G} \max_{D} V(D,G) = \mathbb{E}_{x\sim Pdata(x)}[logD(x)] + \mathbb{E}_{z\sim Pz(z)}\left[log\left(1 - D\big(G(z)\big)\right)\right] \quad (1)$$

$D(x)$ represents the probability predicted by the Discriminator that a sample x is a real image. $G(z)$ denotes the synthetic image generated by the Generator, where Z is a noise input sampled from a prior distribution $P_z(z)$. $P_z(z)$ serves as the noise distribution, while $P_{data}(x)$ represents the target data distribution ($\mathbb{E}$). D aims to maximize$logD(x)$ for real data and $log\left(1 - D\big(G(z)\big)\right)$ for synthetic data, enabling it to distinguish between the two. G the Generator seeks to minimize $log\left(1 - D\big(G(z)\big)\right)$ so that its synthetic data $G(z)$ is accepted by the Discriminator as real data $\left(D\big(G(z)\big) \to 1\right)$. The proposed method for cross-age face verification based on facial development process and landmark feature shown in Fig. 1.

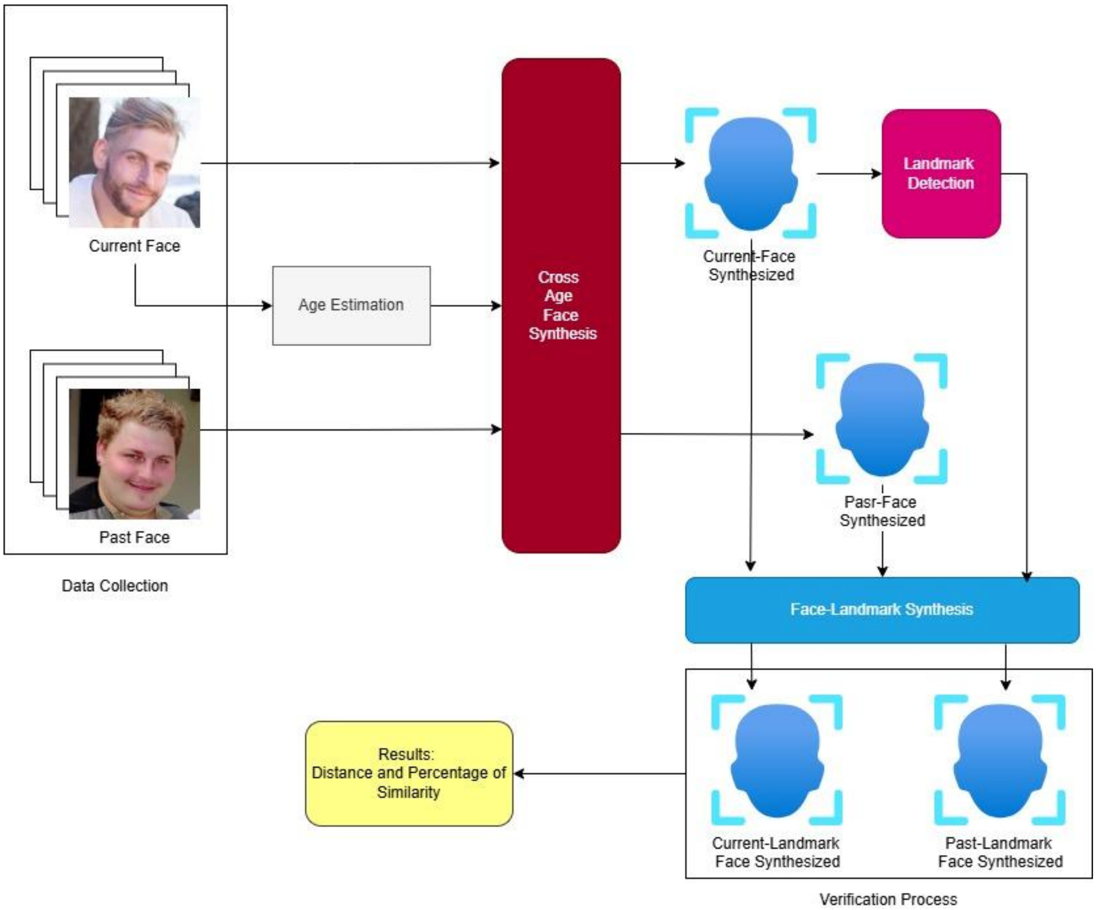

Fig. 1. The proposed method for cross-age face verification based on facial development process and landmark feature

The utilization of GANs in modeling new data has emerged as an innovative approach in cross-age face synthesis research. Cross-age face synthesis focuses on generating realistic facial transformations that simulate natural aging while maintaining the unique identity of the individual.

GANs are designed to map input facial images to target age domains, ensuring that the identity of the individual is preserved throughout the transformation process. The Identity-Preserved Conditional Generative Adversarial Networks framework (Equation (2)) was developed to generate realistic facial transformations for a given target age. This framework ensures that identity features from the original face are retained while the generated face accurately represents the desired age [39].

$$\min_G \max_D \ \mathbb{E}_{x\sim P_x(x)}[logD(x|C_t)] + \mathbb{E}_{y\sim P_y(y)}\left[log\left(1 - D\big(G(y|C_t)\big)\right)\right] \tag{2}$$

In this framework, y represents real faces within the target age group, and x denotes synthetic faces generated by the generator. $P_x(x)$ and $P_y(y)$ are the distributions of synthetic and real faces, respectively. The discriminator $D(x|C_t)$ ensures that real faces yyy are classified correctly as belonging to the target age group. Additionally, D verifies that the generated synthetic faces x align with the target age and appear realistic. The objective function encapsulates the competition between the generator and the discriminator in synthesizing faces. The term $\mathbb{E}_{x\sim P_x(x)}[logD(x|C_t)]$ ensures that real faces x are accurately classified by D. Meanwhile, $\mathbb{E}_{y\sim P_y(y)}\left[log\left(1 - D\big(G(y|C_t)\big)\right)\right]$ ensures that the synthetic faces produced by G are not easily identified as synthetic by D. The generator G aims to create synthetic faces $G(y|C_t))$ that cannot be distinguished from real faces by D. Conversely, the discriminator D strives to differentiate between real faces x and synthetic faces $G(y|C_t))$, while verifying that the faces conform to the target age C_t.

In many cases, obtaining paired young and old facial images of the same individual is challenging. CycleGAN offers a significant advantage for cross-age face synthesis as it eliminates the need for paired data, enabling facial transformations across age groups using unpaired datasets [38], [45]-[47]. The CycleGAN framework employs a cycle-consistency loss, as shown in Equation (3), to ensure that transformations between young and old faces, and vice versa, preserve the individual's identity. This loss enforces consistency in the bidirectional mapping, maintaining the structural and identity features of the original face throughout the transformation process.

$$\mathcal{L}_{cycle} = \mathbb{E}_{x\sim P_{data}(x)}\left[\left\|G_B\big(G_F(x)\big) - x\right\|1\right] + \mathbb{E}_{y\sim P_{data}(y)}\left[\left\|G_F\big(G_B(y)\big) - y\right\|1\right] \tag{3}$$

G_F represents the generator that transforms a face from a younger to an older age, while G_B transforms it back from an older to a younger age. Cycle-consistency ensures that the facial identity remains intact during the bidirectional translation process, preserving the unique features of the individual. The adversarial loss is employed to guarantee that the generated faces align with the desired target age domain. The adversarial loss for CycleGAN can be expressed as follows:

$$\mathcal{L}_{GAN}(G_F, D_Y, X, Y) = \mathbb{E}_{y\sim P_{data}(y)}[logD_Y(y)] + \mathbb{E}_{x\sim P_{data}(x)}[log(1 - D_Y(G_F(x)))] \tag{4}$$

D_Y is the discriminator that ensures the faces generated by G_F resemble those within the older age domain. The total loss in cross-age face synthesis combines both the adversarial loss and the cycle-consistency loss to achieve realistic and identity-preserving transformations. The total loss can be expressed as follows:

$$\mathcal{L}_{Total} = \mathcal{L}_{GAN} + \lambda\mathcal{L}_{Cycle} \tag{5}$$

With λ as a hyperparameter controlling the contribution of the cycle-consistency loss, the model ensures that the final output is not only realistic but also preserves the facial identity. The balance provided by λ is crucial in achieving a trade-off between generating plausible transformations and maintaining individual identity.

Recent literature has integrated attention modules into GAN architectures to focus on facial regions that are particularly sensitive to aging. Liu dkk. (2019) proposed AttentionGAN, which enhances the accuracy of synthesized images by adaptively weighting critical facial features [48]. Additionally, Progressive GANs refine face synthesis by generating images at progressively higher resolutions. Yang et al. (2020) demonstrated that multi-scale GANs can significantly improve the realism and age accuracy of synthesized faces [49]-[51].

StyleGAN (Style-Based Generator Architecture for Generative Adversarial Networks), which was introduced by Karras et al. revolutionized GAN capabilities by enabling the generation of high-quality images with enhanced style control. Age transformation methods based on StyleGAN leverage the rich latent space of a pretrained unconditional GAN to encode real facial images, facilitating significant modifications to facial features and head shapes while preserving the input identity [52]-[56]. Building on this, Alaluf et al. employed a pretrained age regression network to model the aging process continuously as a regression task between the initial and target ages, offering fine-grained and precise control. Furthermore, the method learns through a more disentangled non-linear pathway, enabling advanced editing of the generated images. This approach is superior to state-of-the-art qualitative and quantitative evaluation methods [57].

2.3. Landmark Detection

The cross-age face synthesis for face verification is the primary objective of this study. Face recognition across different age groups is challenging because of significant changes in facial features and structures over time. The verification of the identity of a subject across varying time spans often results in lower accuracy [58]. This challenge becomes even more pronounced with the morphological changes in facial landmarks, which is a key contribution of this research. A robust landmark detection model is essential to initiate this process. Ensemble regression tree models are among the most efficient approaches currently available for landmark detection [59], [60]. The initial shape of the landmarks (S_0) is defined as the mean landmark configuration derived from the training dataset. The model is trained using a loss function that calculates the mean squared error between the predicted landmarks and the ground truth landmarks, ensuring accurate alignment and representation of facial features for subsequent processing.

$$\mathcal{L} = \frac{1}{N}\sum_{i=1}^{N}\left\|S_i^{pred} - S_i^{true}\right\|^2 \tag{6}$$

Here, N represents the total number of image samples in the training dataset. This function ensures that the model minimizes the prediction error of landmark positions during the training process.

2.4. Face-Landmark Synthesis

The final step in the face synthesis method focuses on implementing landmark adjustments after completing the cross-age face synthesis process. Various techniques have been developed in this context. Methods such as face alignment, including affine transformation, Procrustes Analysis, and Helmert Transformation, emphasize rotation, scaling, translation, and shear operations on facial images [61]. However, face-to-face synthesis using techniques like GANnotation offers a more realistic outcome (Sanchez & Valstar, n.d.). These approaches highlight the evolution of facial landmark synthesis methods, which form a critical component of the proposed framework in this research [62].

The method employs a Triple Consistency Loss mechanism to ensure that the synthesized face remains consistent with the input identity, target attributes, and latent space representation. The Image Consistency ($\mathcal{L}_{image}$) measures the consistency of the synthesized face in terms of identity features and visual elements. The Image Consistency can be expressed using the following equation:

$$\mathcal{L}_{image} = \|I - G(I, A)\|^2 \tag{7}$$

I represents the input image, $G(I, A)$ denotes the synthesized image with the target attribute A, and $\|\cdot\|^2$ is the error function, such as the Mean Squared Error (MSE).

Next, Attribute Consistency($\mathcal{L}_{attribute}$) is applied to ensure that the synthesized face accurately reflects the desired target attributes, such as changes in age, expression, or style. ($\mathcal{L}_{attribute}$) can be expressed with the following equation:

$$\mathcal{L}_{attribute} = \left\| C\big(G(I, A)\big) - A \right\|^2 \tag{8}$$

C the attribute predictor model, and A is the target attribute. The third consistency loss, Latent Consistency ($\mathcal{L}_{latent}$) ensures that the latent space representation remains consistent between the input face and the synthesized face. The equation for ($\mathcal{L}_{latent}$) can be represented as follows:

$$\mathcal{L}_{latent} = \left\| Z - E\big(G(I, A)\big) \right\|^2 \tag{9}$$

Here, Z is the latent representation of the input, and E is the encoder that extracts the latent representation from the synthesized face. The Triple Consistency Loss is computed as a combination of the three consistency terms and can be represented by the following equation:

$$\mathcal{L}_{triple} = \lambda_1 \mathcal{L}_{image} + \lambda_2 \mathcal{L}_{attribute} + \lambda_3 \mathcal{L}_{latent} \tag{10}$$

where λ_1, λ_2, λ_3 are weights that determine the relative importance of each component in the overall loss function.

2.5. Verification Process

Face recognition is a technology that allows for the verification of an individual's identity based on distinctive facial features (Syuhada et al., 2018). Currently, advancements in technology and research on face verification have been extensively conducted, achieving nearly perfect accuracy levels. This progress is strongly attributed to the implementation of deep learning methods [63], [64]. OpenCV, an open-source library, has enabled face verification processes with promising accuracy, making it suitable for implementation in specific application projects [65], [66]. This model is also employed to carry out the verification process in this paper. During the evaluation, we compare the verification accuracy of subjects between the proposed method and direct verification. This paper specifically utilizes advanced face verification models to evaluate the performance of the model developed in this study. The models used are ArcFace [67], VGG-Face [68], and Facenet [69].

2.6. Performance Evaluation Metrics

To determine the performance of the proposed method, several standard performance metrics were employed. These metrics provide a general indication of the predictive power of the model according to various aspects, such as verification accuracy, precision, recall, and overall discriminative power. The performance metrics employed in this study are accuracy, precision, recall, F1-score, and AUC-ROC, with each providing distinct information about the model's performance [70], [71].

Accuracy is a fundamental metric that measures the proportion of correctly classified samples relative to the total number of samples. It is computed as follows:

$$Accuracy = \frac{TP + TN}{TP + TN + FP + FN} \tag{11}$$

where TP (True Positive) and TN (True Negative) represent the number of correctly identified positive and negative samples, respectively, and FP (False Positive) and FN (False Negative) denote misclassified instances. Although accuracy is widely used in model evaluation, it can be misleading in scenarios with class imbalance because high accuracy may not necessarily reflect a model's ability to correctly classify minority class instances [72]. To mitigate accuracy limitations, both recall and precision were considered. In contrast, is measured in terms of a positive identified value, and expresses the proportion of positive instances identified out of all identified positive instances. Then, it can be calculated as follows:

$$Precision = \frac{TP}{TP + FP} \tag{12}$$

A high-precision value indicates a lower false positive rate, which is particularly crucial in applications in which false alarms must be minimized [73].

On the other hand, recall, also known as sensitivity, measures the model's ability to correctly identify all relevant instances within the dataset [74]. It is computed as follows:

$$Recall = \frac{TP}{TP + FN} \tag{13}$$

A high recall indicates that the model detects most positive examples, which is an important characteristic in high-stakes applications like disease testing, where a missed positive case (a false negative) can be disastrous [75].

As precision and recall have a trade-off, a balanced measure is provided using the F1 score, taking both of them together into consideration. It is a harmonic mean between precision and recall.

$$F1 - Score = 2 \cdot \frac{Precision \cdot Recall}{Precision + Recall} \tag{14}$$

A higher F1 score indicates a well-balanced model that performs well in terms of both precision and recall, particularly in cases where class imbalance exists [76].

3. Results and Discussion

The implementation of our cross-age face verification model was performed using the Google Colaboratory, leveraging its computational resources. The specifications provided include an Intel(R) Xeon(R) CPU @ 2.00 GHz, a T4 GPU, and 13 GB of RAM. The entire process was conducted virtually using the Chrome browser, ensuring efficient and seamless execution.

3.1. Synthesis Process Experiment

Table 1 presents a visualization of the results for each step of the process. Columns A and B show the two models of facial images representing the past and current faces used to verify their similarity. To facilitate the study, we independently collected a dataset of 200 facial images representing subjects with varying degrees of facial changes due to aging. These variations not only reflect changes in age and significant transformations in facial landmarks, such as transitions from a fuller face to a slimmer face, or vice versa. The proposed dataset provides a comprehensive foundation for evaluating the model's ability to adapt to diverse facial transformations while maintaining verification accuracy. The collected data ensure that the model captures the essential identity-preserving features despite the changes in age and facial structure, which is critical for validating the effectiveness of the proposed method.

In the proposed method, the initial step is Cross-Face Synthesis, which involves generating transformations between facial images. The current age was estimated as a prerequisite for determining the target age for synthesis. Column C in Table 1 represents the age values derived from each row of current faces (Column B). Age was estimated using the DeepFace Python library. This approach was initiated with the command from deepfake import DeepFace, enabling direct access to pre-trained deep learning models for facial analysis. The DeepFace library provides a range of pretrained models capable of detecting and analyzing facial features, including accurate age prediction. Overall, the implementation of age estimation using DeepFace was both effective and efficient. By leveraging its capabilities, age estimation integrates seamlessly into the Cross-Face Synthesis system, where age parameters are critical for guiding the transformation process. This integration ensures that the synthesized faces align accurately with the target age, thereby enhancing the realism and utility of the model in cross-age applications.

Vol. 5, No. 2, 2025, pp. 862-880

Table 1. Visualization of the results at each stage of the proposed method

No	(A) Past Face	(B) Current Face	(C) Curent Age Estimation	(D) Past Cross-Face Synthesis	(E) Current Cross-Face Synthesis	(F) Landmark Detection	(G) Past Face-Landmark Synthesis	(H) Past Face-Landmark Synthesis
1.	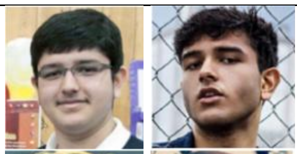		22	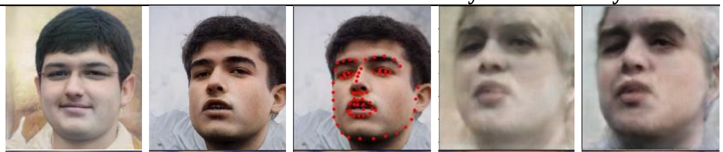				
2.	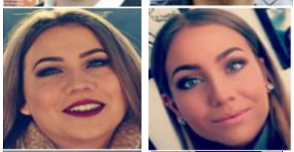		30	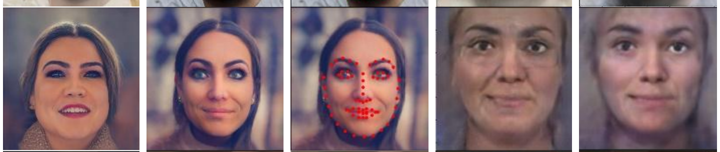				
3.	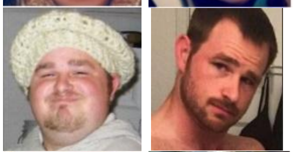		28	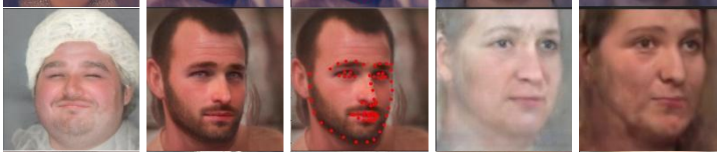				
4.	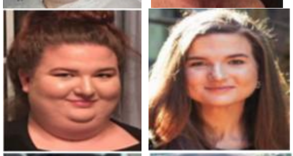		24	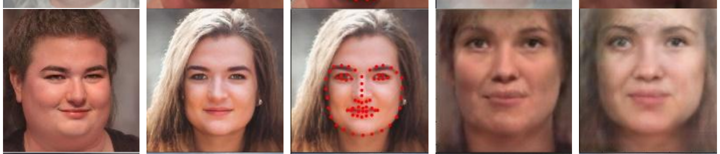				
5.	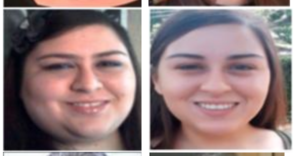		22	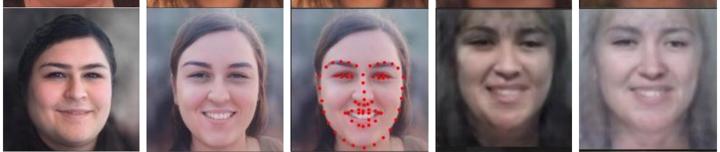				
6.			47	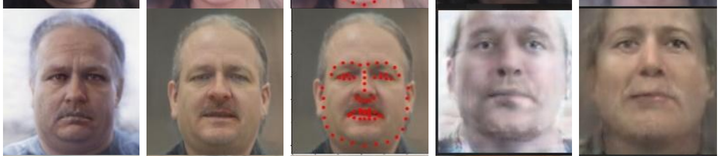				
7.	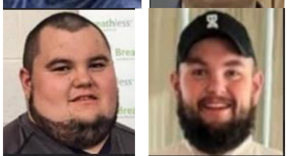		35	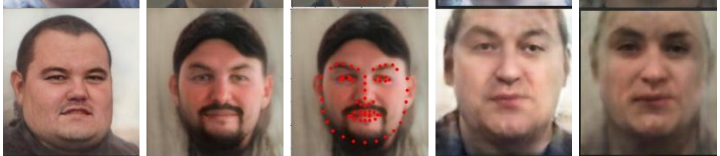				
8.	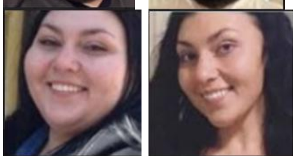		32	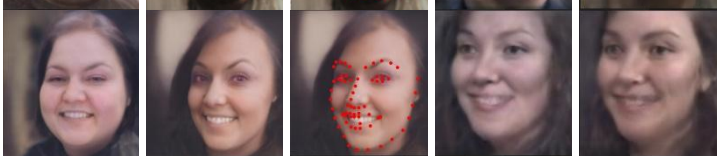				
9.	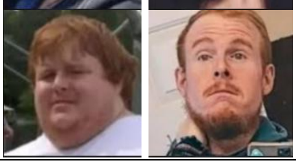		25	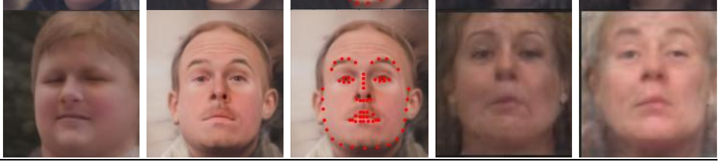				

Column D shows the results of past Cross-Face Synthesis using the GAN method. The GAN synthesizes facial aging from the input image to the estimated age. To enhance the testing scheme, we synthesized the current face (Column B). The assumption here is that a GAN model trained for facial synthesis cannot produce an exact replica of a real face. Thus, both past and current faces must undergo a synthesis under the same conditions. In this context, the current face is synthesized based on the estimated current age derived during the process. This resulted in two synthesized faces, as shown in Columns D and E of Table 1. These two synthesized faces were then used in the testing scheme to compare the outcomes of direct synthesis-based verification with those of the proposed method, which incorporates landmark adjustments. The synthesized faces from Columns D and E are subsequently used in the next phase to align the landmarks according to the objectives of this study. This ensures that both synthesized faces adhere to the methodology proposed in this paper, which emphasizes the significance of landmark-based adjustments to enhance the accuracy and robustness of cross-age face verification.

Face-landmark synthesis was then performed according to the proposed method to adjust the landmark structure of the past-face to accommodate the landmark changes observed in the current-face. This process was applied to the synthesized facial data obtained in Columns D and E of Table 1. The first step involved extracting the landmarks of the current synthesis face (Column E). In this study, facial landmark detection was performed to analyze the geometric structure of the synthesized faces. The landmark prediction method using a model trained on a standard facial dataset. The model identified 68 reference points on the face, representing key features such as the face contour, eyes, nose, and lips. The landmark extraction process begins with facial region detection using a feature-based detection algorithm. After identifying the facial area, the landmark prediction model estimated 66 coordinate points based on the geometric patterns learned during training.

This step ensures accurate representation of facial features and provides a foundation for further landmark alignment adjustments, as per the study objectives. Column F presents the landmark detection results, which highlight the key points obtained on the current synthesis face. Visual validation of these landmarks demonstrates alignment with the original facial structure, which serves as the basis for the final synthesis of the proposed method. This indicates that the prediction model effectively adapts to the complex features present in the synthesized faces. The detected landmarks are then used to align the landmark structure of the Past-Synthesis Face (Column D) with that of the Current-Synthesis Face (Column E). To realize this, we employed a GANnotation model that can generate highly realistic facial representations. Ultimately, the synthesis process results in the Past-Landmark Synthesized Face (Column H) and the Current-Landmark Synthesized Face, both forming the final synthesized faces. These were then verified for similarity, demonstrating the efficacy of our proposed method for cross-age face synthesis and verification.

3.2. Distance Verification Rate of Experiment

The results of each step are presented in Table 1. To evaluate the impact of the proposed method on cross-age face verification, quantitative testing was conducted. The quantitative evaluation was performed by analyzing the changes in the Distance Verification Rate (DVR) across the synthesized face outputs generated by the proposed cross-age verification method. Table 2 provides a detailed description of the quantitative testing conducted, illustrating the comparative results and the effectiveness of the proposed approach.

The results of each step are presented in Table 1. To evaluate the impact of the proposed method on cross-age face verification, quantitative testing was conducted. The quantitative evaluation was performed by analyzing the changes in the Distance Verification Rate (DVR) across the synthesized face outputs generated by the proposed cross-age verification method. Table 2 provides a detailed description of the quantitative testing conducted, illustrating the comparative results and the effectiveness of the proposed approach.

We conducted a series of experiments to evaluate the impact of the Distance Verification Rate (DVR) at each stage of the proposed method. The first scheme, A → B, involved verifying the original images of each subject (Column A and B in Table 1) to establish the baseline verification rate before applying the proposed method. Next, D → E was conducted to assess the DVR between the Past-Synthesis Face and the Current-Synthesis Face, both generated based on the estimated age. The third scheme, B → G, evaluates the verification rate between the Original Current Face (Column B) and the Past-Landmark Synthesis Face (Column G), providing insight into how well the proposed method aligns the synthesized past face with the original current face. Similarly, E → G was performed to verify the Current-Synthesis Face (Column E) with the Current-Landmark Synthesis Face (Column

G), measuring the consistency of the synthesis process. Lastly, G → H represents the outcome of the proposed method, where verification was conducted between the detected landmarks from the Current-Synthesis Face (Column F) and the final Current-Landmark Synthesis Face (Column G). These schemes collectively provide a comprehensive evaluation of the proposed method's effectiveness in improving cross-age face verification by analyzing DVR changes at various stages.

Table 2. Distance verification rate from the conducted experiments

Sample Subject	Distance Verification Rate of Experiment Model				
	A→B	**D→E**	**B→G**	**E→G**	**G→H**
1	0.5511	0.5660	0.6940	0.7475	**0.4452**
2	0.5130	0.5013	0.7217	0.6986	**0.4685**
3	0.4607	0.5491	0.7267	0.7275	**0.3777**
4	0.4496	0.5199	0.6393	0.6525	**0.3713**
5	0.5617	0.5528	0.7162	0.7232	**0.3106**
6	0.5925	0.5821	0.5538	0.6376	**0.3125**
7	0.5355	0.5955	0.7359	0.7491	**0.5041**
8	0.5621	0.5375	0.7972	0.7568	**0.4816**
9	0.6476	0.6657	0.6269	0.6949	**0.4089**
10	0.6109	0.5456	0.6621	0.6890	**0.4211**
11	0.5057	0.5248	0.5953	0.5929	**0.3729**
12	0.6761	0.5607	0.5708	0.5788	**0.3794**
13	0.5487	0.5123	0.7404	0.7413	**0.4110**
14	0.5846	0.5853	0.6778	0.6818	**0.4127**
15	0.4477	0.5461	0.8051	0.7513	**0.4147**
16	0.5228	0.5458	0.5574	0.5378	**0.3927**
17	0.5854	0.5965	0.6139	0.6539	**0.3620**
18	0.6743	0.8499	0.7282	0.6594	**0.4510**
19	0.4976	0.5570	0.7774	0.6813	**0.4177**
20	0.5457	0.6684	0.6152	0.6076	**0.4061**
21	0.5625	0.5275	0.6125	0.6250	**0.3475**
22	0.5436	0.6325	0.8215	0.7493	**0.4941**
23	0.4995	0.5461	0.7559	0.6519	**0.4386**
24	0.4752	0.6128	0.6556	0.6619	**0.3999**
25	0.4909	0.5237	0.5553	0.5818	**0.3977**
26	0.5994	0.6658	0.5657	0.6112	**0.5731**
27	0.5855	0.5098	0.6764	0.6615	**0.3657**
28	0.5819	0.6930	0.7571	0.7451	**0.3795**
29	0.5144	0.6631	0.7448	0.5979	**0.4530**
30	0.5199	0.5301	0.5961	0.6279	**0.4940**
31	0.4711	0.5512	0.7167	0.6859	**0.4693**
32	0.5937	0.7124	0.7698	0.8410	**0.4692**
33	0.5612	0.5323	0.6919	0.6930	**0.4992**
34	0.5566	0.4343	0.7457	0.6451	**0.5160**
35	0.6225	0.7582	0.7250	0.6897	**0.5162**
36	0.6092	0.6333	0.7196	0.6983	**0.4122**
37	0.5563	0.6394	0.6587	0.6434	**0.5457**
38	0.5423	0.6368	0.6326	0.6312	**0.4881**
39	0.3619	0.4997	0.5613	0.5496	**0.2925**
40	0.5288	0.4728	0.7009	0.6267	**0.3096**
41	0.5355	0.5955	0.7359	0.7491	**0.5041**
42	0.5621	0.5375	0.7972	0.7568	**0.4816**
43	0.6476	0.6657	0.6269	0.6949	**0.4089**
44	0.6666	0.6541	0.7802	0.7090	**0.6180**
45	0.5032	0.6123	0.6541	0.6357	**0.4508**

The Distance Verification Rate (DVR) results presented in Table 1 demonstrate the effectiveness of the proposed method in addressing cross-age face verification challenges. Baseline verification between original past and current faces (A → B) exhibits relatively high DVR values, such as 0.5511 for Sample 1 and 0.6476 for Sample 9, reflecting the inherent difficulty of verifying faces across significant age-related changes. In contrast, the synthesized face comparison (D → E), with DVR values of 0.5660 (Sample 1) and 0.6657 (Sample 9), shows moderate improvement, indicating the ability of the synthesis process to reduce age discrepancies. Verification between the original current face and the past-landmark synthesis face (B → G), as evidenced by values like 0.6940 (Sample 1) and 0.6269 (Sample 9), further underscores the alignment achieved through landmark adjustments. Similarly, the comparison between synthesized current faces (E → G) yielded DVR values of 0.7475 (Sample 1) and 0.6949 (Sample 9), demonstrating consistency in the synthesis process. Notably, the proposed method (G → H) achieved the lowest DVR values, including 0.4452 for Sample 1 and 0.4089 for Sample 9, confirming its ability to effectively align past and current faces while preserving identity. These findings validate the proposed approach as a robust solution for improving cross-age face verification accuracy.

3.3. Verification Rate of Experiment

In the evaluation stage presented in Table 3, we focused on analyzing additional pairs of cross-age facial images using both direct verification and the proposed method. The direct verification approach failed to verify several pairs due to low similarity percentages and high feature distances. For instance, pair 6 achieved only a 32.57% similarity rate with a feature distance of 0.6743, resulting in a "not verified" status. However, the proposed method improved the similarity percentage to 54.90% and reduced the feature distance to 0.4510, thereby successfully verifying the pair. These results highlight the limitations of direct verification, particularly when dealing with significant variations caused by aging.

The proposed method consistently outperformed the limitations of direct verification. For pair 5, the similarity percentage increased from 41.46% to 63.80%, and the feature distance significantly decreased from 0.5854 to 0.3620. Similar trends were observed in other pairs, such as pair 7, where the similarity percentage improved from 35.24% to 59.11%, thereby enabling successful verification. This demonstrates that the proposed method can address the dynamic changes in facial features and produce more reliable results.

This stage of evaluation further confirms the reliability of the proposed cross-age face verification method. By effectively addressing the challenges posed by aging and structural transformations in facial features, the proposed method provides a robust solution to verify previously unverifiable facial image pairs using direct methods. The success of the proposed method across a variety of scenarios underscores its potential for implementation in practical applications, particularly in security, forensic analysis, and other areas requiring accurate facial recognition over time.

3.4. Performance Evaluation of Cross-Age Face Verification Model

In this section, we discuss the performance of various face verification models in terms of cross-age face verification. The performance is divided into two categories: direct verification and the proposed cross-age verification scheme. In both cases, the comparative performance values of the ArcFace, VGG-Face, and Facenet models are presented in Table 4.

The direct verification performance shows the baseline performance of the model without utilizing the proposed cross-age verification scheme. ArcFace obtained the best accuracy 82.64 and F1-score 79.64 compared to VGG-Face and Facenet. However, Facenet demonstrated relatively poor recall 37.88 with high precision 92.59, indicating failure in effectively distinguishing between true positive cases.

When the new cross-age verification method is implemented, all of the models' performance is boosted. ArcFace still holds its position with a performance of 86.02 accuracy and 81.23 F1-score. VGG-Face takes a close second with 80.57 accuracy and 79.68 F1-score. Facenet, which had the poorest performance, showed a significant improvement in recall, ranging from 37.88 to 57.93, indicating the efficacy of the new technique.

The results demonstrate that the proposed cross-age verification scheme effectively enhances face verification model performance in terms of all performance metrics and recall improvements. In particular, for Facenet, we validated that the difficulty of identifying correct positive cases in cross-age cases is reduced with the proposed scheme. ArcFace consistently outperforms all other models and is therefore most reliable for cross-age face verification. In summary, the proposed method significantly improves cross-age face verification and offers a real-world solution for age-related face variation challenges. There is potential for future work to generalize the proposed technique to other demographics and settings.

Table 3. Direct verification and proposed method verification experiment

No	(A) Past Face	(B) Current Face	Direct Verification			Proposed Method Verification		
			Percent Rate	Distance	Status	Percent Rate	Distance	Status
1			44.89	0.5511	Verified	55.48	0.4452	Verified
2	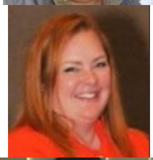		40.75	0.5925	Verified	68.75	0.3125	Verified
3		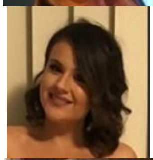	55.04	0.4496	Verified	62.87	0.3713	Verified
4			32.39	0.6761	Not Verified	62.06	0.3794	Verified
5		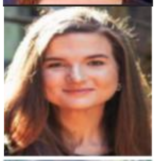	41.46	0.5854	Not Verified	63.80	0.3620	Verified
6	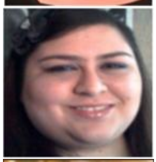		32.57	0.6743	Not Verified	54.90	0.4510	Verified
7			35.24	0.6476	Not Verified	59.11	0.4089	Verified
8	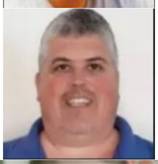		35.11	0.6489	Not Verified	40.42	0.5958	Verified
9			29.69	0.7031	Not Verified	48.19	0.5181	Verified

Table 4. Direct verification and proposed method verification experiment

Model	Accuracy	F1-score	Precision	Recall	AUC
Direct Verification					
ArcFace	0.826415	0.79646	0.957447	0.681818	0.825871
VGG-Face	0.762264	0.704225	0.925926	0.568182	0.761535
Facenet	0.675472	0.537634	0.925926	0.378788	0.674356
Proposed Method Cross-Age Verification					
ArcFace	0.860215	0.812345	0.86258	0.720512	0.843789
VGG-Face	0.805732	0.796843	0.810512	0.790658	0.802147
Facenet	0.744828	0.694215	0.865979	0.57931	0.744828

4. Conclusion

Cross-age face verification is an emerging research challenge that has gained significant attention. The primary challenge lies in determining whether a current facial image can be recognized or verified compared to facial data collected over a specific time interval. This paper proposes a Cross-Age Face Verification Method Based on the Facial Development Process, integrating a Deep Learning Approach Using Generative Adversarial Networks (GAN) with Landmark Features. The proposed method overcomes limitations, such as difficulties in handling facial regions affected by accessories, and achieves consistent aging effects in specific facial areas. GAN is the primary development framework to synthesize facial images using age and landmark parameters. The goal of this study is to design a facial development model that combines GAN with advanced facial landmark detection modules. Once past facial images are synthesized into new facial data models, these synthesized models are then verified against the current facial images to assess their similarity levels. The dataset used in this study comprised cross-age facial images. Each subject's facial data is collected based on photographs taken at specific age intervals, such as adolescence, adulthood, and old age. The facial data were gathered via online searches using resources such as Google or social media platforms. Public figures, officials, and celebrities provide readily available sources of facial data, making them suitable candidates for inclusion in the dataset used in this research.

The experiments involved verifying the original facial data and synthesized data generated using the proposed method. The experimental process was conducted in several stages, beginning with age-based face synthesis using the GAN method, followed by applying GANnotation to refine the synthesized faces by aligning them with the updated landmark structure of the current face. To evaluate the impact of the proposed method, multiple verification schemes were performed, including direct verification between the original past and current faces and verification of synthesized faces before and after incorporating landmark adjustments.

The results demonstrate that the proposed cross-age synthesis method, combined with landmark features, significantly reduces the Distance Verification Rate (DVR) between two faces with substantial age gaps and landmark variations. In cases where direct verification resulted in invalid outcomes due to distances exceeding the defined threshold, the proposed method successfully verified these subjects. Generally, the proposed method effectively achieves its intended objective of verifying two facial images of a subject with varying age ranges and landmark structures. Further research is required to expand the dataset and increase the model complexity, with the aim of improving the evaluation metrics and preparing the model for real-world applications.

The cross-age face verification model evaluation demonstrated that the proposed performance was significantly improved in all tested models, i.e., ArcFace, VGG-Face, and Facenet. The proposed performance is maximized for essential metrics like accuracy, F1-score, precision, recall, and AUC, by overcoming age-related face variation. ArcFace consistently performs better than all other models, with its high performance in both direct and cross-age conditions indicating its efficacy in both scenarios. These findings validate the effectiveness of the proposed face verification technology and thus its potential in mitigating age-related face variation in biometric systems.

Author Contribution: All authors contributed equally to the main contributor to this paper. All authors read and approved the final paper.

Acknowledgement: This research was supported by the Indonesian Ministry of Education, Culture, Research, and Technology (KEMENDIKBUDRISTEK) through the BIMA Program and the Beginner Lecturer Research Scheme (Penelitian Dosen Pemula) in 2024.

Conflicts of Interest: The authors declare no conflict of interest.

References

[1] K. Adeshara and V. Elangovan, “Face recognition using PCA integrated with Delaunay triangulation,” *Computer Science & Information Technology*, pp. 321-331, 2020, https://doi.org/10.5121/csit.2020.101424.

[2] M. Balazia, S. L. Happy, F. Brémond and A. Dantcheva, "How Unique Is a Face: An Investigative Study," *2020 25th International Conference on Pattern Recognition (ICPR)*, pp. 7066-7071, 2021, https://doi.org/10.1109/ICPR48806.2021.9412446.

[3] F. Syuhada, I. G. P. S. Wijaya, and F. Bimantoro, “Pengenalan Wajah Untuk Sistem Kehadiran Menggunakan Metode Eigenface and Euclidean Distance,” *Journal of Computer Science and Informatics Engineering*, vol. 2, no. 1, pp. 64-69, 2018, https://doi.org/10.29303/jcosine.v2i1.74.

[4] G. Sharma, G. Jaswal, A. Nigam and R. Ramachandra, "FH-SSTNet: Forehead Creases based User Verification using Spatio-Spatial Temporal Network," *2024 12th International Workshop on Biometrics and Forensics (IWBF)*, pp. 1-6, 2024, https://doi.org/10.1109/IWBF62628.2024.10593960.

[5] B.-N. Kang, Y. Kim, and D. Kim, “Pairwise relational networks using local appearance features for face recognition,” *Computer Vision – ECCV 2018*, pp. 646–663, 2018, https://doi.org/10.1007/978-3-030-01216-8_39.

[6] L. Qinjun, C. Tianwei, Z. Yan, W. Yuying, “Facial recognition technology: a comprehensive overview,” *Academic Journal of Computing & Information Science*, vol. 6, no. 7, pp. 15-26, 2023, https://francis-press.com/papers/11241.

[7] Z. -M. Chen, X. -S. Wei, P. Wang and Y. Guo, "Learning Graph Convolutional Networks for Multi-Label Recognition and Applications," *IEEE Transactions on Pattern Analysis and Machine Intelligence*, vol. 45, no. 6, pp. 6969-6983, 2023, https://doi.org/10.1109/TPAMI.2021.3063496.

[8] G. M. Gouaya, E. F. D. Goufo, P. Kubeka, “Enhancing Facial Recognition Models Accuracy Through Dimension Reduction Techniques,” *Amos, Enhancing Facial Recognition Models Accuracy Through Dimension Reduction Techniques*, 2024, https://dx.doi.org/10.2139/ssrn.5056730.

[9] S. Z. Li, A. K. Jain, “Handbook of face recognition,” *Springer London*, 2011, https://doi.org/10.1007/978-0-85729-932-1.

[10] L. Liu, C. Xiong, H. Zhang, Z. Niu, M. Wang and S. Yan, "Deep Aging Face Verification With Large Gaps," *IEEE Transactions on Multimedia*, vol. 18, no. 1, pp. 64-75, 2016, https://doi.org/10.1109/TMM.2015.2500730.

[11] M. M. Sawant, K. M. Bhurchandi, “Age invariant face recognition: a survey on facial aging databases, techniques and effect of aging,” *Artificial Intelligence Review*, vol. 52, pp. 981-1008, 2019, https://doi.org/10.1007/s10462-018-9661-z.

[12] K. Ricanek and E. Boone, "The effect of normal adult aging on standard PCA face recognition accuracy rates," *Proceedings. 2005 IEEE International Joint Conference on Neural Networks, 2005.*, vol. 4, pp. 2018-2023, 2005, https://doi.org/10.1109/IJCNN.2005.1556210.

[13] H. Yang, D. Huang, Y. Wang and A. K. Jain, "Learning Continuous Face Age Progression: A Pyramid of GANs," *IEEE Transactions on Pattern Analysis and Machine Intelligence*, vol. 43, no. 2, pp. 499-515, 2021, https://doi.org/10.1109/TPAMI.2019.2930985.

[14] M. Grimmer, R. Ramachandra and C. Busch, "Deep Face Age Progression: A Survey," *IEEE Access*, vol. 9, pp. 83376-83393, 2021, https://doi.org/10.1109/ACCESS.2021.3085835.

[15] M. RajaBabu, K. Srinivas and H. R. Sankar, "Survey on Age Invariant Face Recognition Techniques," *2022 5th International Conference on Contemporary Computing and Informatics (IC3I)*, pp. 2147-2153, 2022, https://doi.org/10.1109/IC3I56241.2022.10072620.

[16] A. R. Joshi, X. Suau, N. Sivakumar, L. Zappella, and N. Apostoloff, “Fair SA: Sensitivity Analysis for Fairness in Face Recognition,” *arXiv*, 2022, https://doi.org/10.48550/arXiv.2202.03586.

[17] I. Sarridis, C. Koutlis, S. Papadopoulos, and C. Diou, “Towards Fair Face Verification: An In-depth Analysis of Demographic Biases,” *arXiv*, 2023, https://doi.org/10.48550/arXiv.2307.10011.

[18] H. Yassin, S. Hoque and F. Deravi, "Impact Of Age And Ageing On Face Recognition Performance," *2019 IEEE Asia-Pacific Conference on Computer Science and Data Engineering (CSDE)*, pp. 1-7, 2019, https://doi.org/10.1109/CSDE48274.2019.9162417.

[19] W. Yao, M. A. Farooq, J. Lemley and P. Corcoran, "Synthetic Face Ageing: Evaluation, Analysis and Facilitation of Age-Robust Facial Recognition Algorithms," *IEEE Transactions on Biometrics, Behavior, and Identity Science*, 2025, https://doi.org/10.1109/TBIOM.2025.3536622.

[20] N. Ramanathan and R. Chellappa, "Face verification across age progression," *2005 IEEE Computer Society Conference on Computer Vision and Pattern Recognition (CVPR'05)*, vol. 2, pp. 462-469, 2005, https://doi.org/10.1109/CVPR.2005.153.

[21] H. Ling, S. Soatto, N. Ramanathan and D. W. Jacobs, "Face Verification Across Age Progression Using Discriminative Methods," *IEEE Transactions on Information Forensics and Security*, vol. 5, no. 1, pp. 82-91, 2010, https://doi.org/10.1109/TIFS.2009.2038751.

[22] G. Mahalingam and C. Kambhamettu, “Face verification of age separated images under the influence of internal and external factors,” *Image and Vision Computing*, vol. 30, no. 12, pp. 1052–1061, 2012, https://doi.org/10.1016/j.imavis.2012.10.003.

[23] T. Wu, P. Turaga and R. Chellappa, "Age Estimation and Face Verification Across Aging Using Landmarks," *IEEE Transactions on Information Forensics and Security*, vol. 7, no. 6, pp. 1780-1788, 2012, https://doi.org/10.1109/TIFS.2012.2213812.

[24] D. Yadav, M. Vatsa, R. Singh and M. Tistarelli, "Bacteria Foraging Fusion for Face Recognition across Age Progression," *2013 IEEE Conference on Computer Vision and Pattern Recognition Workshops*, pp. 173-179, 2013, https://doi.org/10.1109/CVPRW.2013.33.

[25] L. Du and H. Ling, "Cross-age face verification by coordinating with cross-face age verification," *2015 IEEE Conference on Computer Vision and Pattern Recognition (CVPR)*, pp. 2329-2338, 2015, https://doi.org/10.1109/CVPR.2015.7298846.

[26] S. N. Gowda, "Face verification across age progression using facial feature extraction," *2016 International Conference on Signal and Information Processing (IConSIP)*, pp. 1-5, 2016, https://doi.org/10.1109/ICONSIP.2016.7857437.

[27] R. S. Ghiass, O. Arandjelović, A. Bendada, X. Maldague, “Infrared face recognition: A comprehensive review of methodologies and databases,” *Pattern Recognition*, vol. 47, no. 9, pp. 2807-2824, 2014, https://doi.org/10.1016/j.patcog.2014.03.015.

[28] A. J. Shepley, “Deep Learning for Face Recognition: A Critical Analysis,” *Computer Vision and Pattern Recognition*, 2020, https://doi.org/10.48550/arXiv.1907.12739.

[29] W. Liu, W. Chen, Y. Zhu and L. Shen, "SATGAN: Augmenting Age Biased Dataset for Cross-Age Face Recognition," *2020 25th International Conference on Pattern Recognition (ICPR)*, pp. 1368-1375, 2021, https://doi.org/10.1109/ICPR48806.2021.9412084.

[30] Y. Wang, S. Bai, X. Wan and F. Chen, "Cross-age face recognition for face images in digital archives," *2023 4th International Seminar on Artificial Intelligence, Networking and Information Technology (AINIT)*, pp. 315-319, 2023, https://doi.org/10.1109/AINIT59027.2023.10212553.

[31] C. N. Duong, K. G. Quach, K. Luu, T. H. N. Le and M. Savvides, "Temporal Non-volume Preserving Approach to Facial Age-Progression and Age-Invariant Face Recognition," *2017 IEEE International Conference on Computer Vision (ICCV)*, pp. 3755-3763, 2017, https://doi.org/10.1109/ICCV.2017.403.

[32] A. Radford, L. Metz, and S. Chintala, “Unsupervised representation learning with deep convolutional generative adversarial networks,” *Machine Learning*, 2016, https://doi.org/10.48550/arXiv.1511.06434.

[33] M. Mathieu, C. Couprie, and Y. LeCun, “Deep multi-scale video prediction beyond mean square error,” *Machine Learning*, 2016, https://doi.org/10.48550/arXiv.1511.05440.

[34] Y. Taigman, A. Polyak, and L. Wolf, “Unsupervised cross-domain image generation,” *Computer Vision and Pattern Recognition*, 2017, https://doi.org/10.48550/arXiv.1611.02200.

[35] I. Gulrajani, F. Ahmed, M. Arjovsky, V. Dumoulin, A. Courville, “Improved Training of Wasserstein GANs,” *Machine Learning*, 2017, https://doi.org/10.48550/arXiv.1704.00028.

[36] M. Mirza, S. Osindero, “Conditional Generative Adversarial Nets,” *Machine Learning*, pp. 1–7, 2014, https://doi.org/10.48550/arXiv.1411.1784.

[37] S. Reed, Z. Akata, X. Yan, L. Logeswaran, B. Schiele, H. Lee, “Generative Adversarial Text to Image Synthesis,” *Machine Learning*, 2016, https://doi.org/10.48550/arXiv.1605.05396.

[38] J.-Y. Zhu, T. Park, P. Isola, and A. A. Efros, “Unpaired Image-to-Image Translation using Cycle-Consistent Adversarial Networks,” *Computer Vision and Pattern Recognition*, 2020, https://doi.org/10.48550/arXiv.1703.10593.

[39] X. Tang, Z. Wang, W. Luo and S. Gao, "Face Aging with Identity-Preserved Conditional Generative Adversarial Networks," *2018 IEEE/CVF Conference on Computer Vision and Pattern Recognition*, pp. 7939-7947, 2018, https://doi.org/10.1109/CVPR.2018.00828.

[40] P. K. Chandaliya and N. Nain, “AW-GAN: face aging and rejuvenation using attention with wavelet GAN,” *Neural Computing and Applications*, vol. 35, no. 3, pp. 2811–2825, 2023, https://doi.org/10.1007/s00521-022-07721-4.

[41] P. Siritanawan, H. Ichikawa and K. Kotani, "Facial Age Progression using Conditional Generative Adversarial Network with Heritable Visual Features," *2021 IEEE International Conference on Systems, Man, and Cybernetics (SMC)*, pp. 1449-1454, 2021, https://doi.org/10.1109/SMC52423.2021.9659067.

[42] S. Jeon, P. Lee, K. Hong and H. Byun, "Continuous Face Aging Generative Adversarial Networks," *ICASSP 2021 - 2021 IEEE International Conference on Acoustics, Speech and Signal Processing (ICASSP)*, pp. 1995-1999, 2021, https://doi.org/10.1109/ICASSP39728.2021.9414429.

[43] T. -J. Liu and C. -C. Wang, "Face Aging Synthesis by Deep Cycle Generative Adversarial Networks and Bias Loss," *IEEE Access*, vol. 12, pp. 166439-166458, 2024, https://doi.org/10.1109/ACCESS.2024.3493376.

[44] I. Goodfellow *et al*., “Generative adversarial networks,” *Communications of the ACM*, vol. 63, no. 11, pp. 139–144, 2014, https://doi.org/10.1145/3422622.

[45] Y. He, K. P. Seng and L. M. Ang, "CycleGAN*: Collaborative AI Learning With Improved Adversarial Neural Networks for Multimodalities Data," *IEEE Transactions on Artificial Intelligence*, vol. 5, no. 11, pp. 5616-5629, 2024, https://doi.org/10.1109/TAI.2024.3432856.

[46] T. An and C. Joo, "CycleGANAS: Differentiable Neural Architecture Search for CycleGAN," *2024 IEEE/CVF Conference on Computer Vision and Pattern Recognition Workshops (CVPRW)*, pp. 1655-1664, 2024, https://doi.org/10.1109/CVPRW63382.2024.00172.

[47] D. Lin, B. Tondi, B. Li and M. Barni, "A CycleGAN Watermarking Method for Ownership Verification," *IEEE Transactions on Dependable and Secure Computing*, 2024, https://doi.org/10.1109/TDSC.2024.3424900.

[48] Z. He, W. Zuo, M. Kan, S. Shan and X. Chen, "AttGAN: Facial Attribute Editing by Only Changing What You Want," *IEEE Transactions on Image Processing*, vol. 28, no. 11, pp. 5464-5478, 2019, https://doi.org/10.1109/TIP.2019.2916751.

[49] P. K. Chandaliya and N. Nain, "Child Face Age Progression and Regression using Self-Attention Multi-Scale Patch GAN," *2021 IEEE International Joint Conference on Biometrics (IJCB)*, pp. 1-8, 2021, https://doi.org/10.1109/IJCB52358.2021.9484329.

[50] J. Li, H. Huo, C. Li, R. Wang and Q. Feng, "AttentionFGAN: Infrared and Visible Image Fusion Using Attention-Based Generative Adversarial Networks," *IEEE Transactions on Multimedia*, vol. 23, pp. 1383-1396, 2021, https://doi.org/10.1109/TMM.2020.2997127.

[51] H. Tan, B. Yin, K. Xu, H. Wang, X. Liu and X. Li, "Attention-Bridged Modal Interaction for Text-to-Image Generation," *IEEE Transactions on Circuits and Systems for Video Technology*, vol. 34, no. 7, pp. 5400-5413, 2024, https://doi.org/10.1109/TCSVT.2023.3347971.

[52] T. Karras, S. Laine and T. Aila, "A Style-Based Generator Architecture for Generative Adversarial Networks," *2019 IEEE/CVF Conference on Computer Vision and Pattern Recognition (CVPR)*, pp. 4396-4405, 2019, https://doi.org/10.1109/CVPR.2019.00453.

[53] T. Karras, S. Laine, M. Aittala, J. Hellsten, J. Lehtinen, and T. Aila, "Analyzing and improving the image quality of StyleGAN," *Computer Vision and Pattern Recognition*, 2020, https://doi.org/10.48550/arXiv.1912.04958.

[54] H. Jia *et al*., "BlazeStyleGAN: A Real-Time On-Device StyleGAN," *2023 IEEE/CVF Conference on Computer Vision and Pattern Recognition Workshops (CVPRW)*, pp. 4690-4694, 2023, https://doi.org/10.1109/CVPRW59228.2023.00495.

[55] S. Park and Y. -G. Shin, "Rethinking Image Skip Connections in StyleGAN2," *IEEE Transactions on Neural Networks and Learning Systems*, 2024, https://doi.org/10.1109/TNNLS.2024.3495633.

[56] A. Suwała, B. Wójcik, M. Proszewska, J. Tabor, P. Spurek and M. Śmieja, "Face Identity-Aware Disentanglement in StyleGAN," *2024 IEEE/CVF Winter Conference on Applications of Computer Vision (WACV)*, pp. 5210-5219, 2024, https://doi.org/10.1109/WACV57701.2024.00514.

[57] Y. Alaluf, O. Patashnik, and D. Cohen-Or, "Only a matter of style: Age transformation using a style-based regression model," *ACM Transactions on Graphics*, vol. 40, no. 4, pp. 1-12, 2021, https://doi.org/10.1145/3450626.3459805.

[58] L. Sexton *et al*., "Recognizing newly learned faces across changes in age," *Visual Cognition*, vol. 31, no. 8, pp. 617-632, 2024, https://doi.org/10.1080/13506285.2024.2315813.

[59] V. Kazemi and J. Sullivan, "One millisecond face alignment with an ensemble of regression trees," *2014 IEEE Conference on Computer Vision and Pattern Recognition*, pp. 1867-1874, 2014, https://doi.org/10.1109/CVPR.2014.241.

[60] M. Jeong, JoonYoung Kwak, B. C. Ko and J. Nam, "Facial landmark detection based on an ensemble of local weighted regressors during real driving situation," *2016 23rd International Conference on Pattern Recognition (ICPR)*, pp. 2198-2203, 2016, https://doi.org/10.1109/ICPR.2016.7899962.

[61] C. Á. Casado and M. B. López, "Real-time face alignment: evaluation methods, training strategies and implementation optimization," *Journal of Real-Time Image Processing*, vol. 18, no. 6, pp. 2239–2267, 2021, https://doi.org/10.1007/s11554-021-01107-w.

[62] E. Sanchez and M. Valstar, "Triple consistency loss for pairing distributions in GAN-based face synthesis," *Computer Vision and Pattern Recognition*, 2018, https://doi.org/10.48550/arXiv.1811.03492.

[63] A. Ali, M. Testa, T. Bianchi, and E. Magli, "BioMetricNet: Deep Unconstrained Face Verification through Learning of Metrics Regularized onto Gaussian Distributions," *Computer Vision and Pattern Recognition*, 2020, https://doi.org/10.48550/arXiv.2008.06021.

[64] M. de A. Angeloni and H. Pedrini, "Improving Makeup Face Verification by Exploring Part-Based Representations," *Computer Vision and Pattern Recognition*, 2021, https://doi.org/10.48550/arXiv.2101.07338.

[65] A. Abdelbar, "Face Recognition Using OpenCV and Python: A Review," *International Journal of Scientific and Research Publications*, vol. 14, no. 1, 2024, https://www.ijsrp.org/research-paper-0124.php?rp=P14513223.

[66] Z. Zhu and Y. Cheng, "Application of attitude tracking algorithm for face recognition based on OpenCV in the intelligent door lock," *Computer Communications*, vol. 154, no. 900, pp. 390–397, 2020, https://doi.org/10.1016/j.comcom.2020.02.003.

[67] J. Deng, J. Guo, J. Yang, N. Xue, I. Kotsia and S. Zafeiriou, "ArcFace: Additive Angular Margin Loss for Deep Face Recognition," *IEEE Transactions on Pattern Analysis and Machine Intelligence*, vol. 44, no. 10, pp. 5962-5979, 2022, https://doi.org/10.1109/TPAMI.2021.3087709.

[68] M. Wang, W. Deng, "Deep face recognition: A survey," *Neurocomputing*, vol. 429, pp. 215-244, 2021, https://doi.org/10.1016/j.neucom.2020.10.081.

[69] F. Schroff, D. Kalenichenko and J. Philbin, "FaceNet: A unified embedding for face recognition and clustering," *2015 IEEE Conference on Computer Vision and Pattern Recognition (CVPR)*, pp. 815-823, 2015, https://doi.org/10.1109/CVPR.2015.7298682.

[70] M. Sokolova and G. Lapalme, "A systematic analysis of performance measures for classification tasks," *Information Processing & Management*, vol. 45, no. 4, pp. 427–437, 2009, https://doi.org/10.1016/j.ipm.2009.03.002.

[71] D. M. W. Powers, "Evaluation: from precision, recall, and F-measure to ROC, informedness, markedness & correlation," *Machine Learning*, 2020, https://doi.org/10.48550/arXiv.2010.16061.

[72] A. Fernández, S. Garcia, F. Herrera, and N. V Chawla, "SMOTE for learning from imbalanced data: progress and challenges, marking the 15-year anniversary," *Journal of Artificial Intelligence Research*, vol. 61, pp. 863–905, 2018, https://doi.org/10.1613/jair.1.11192.

[73] M. Bekkar, H. K. Djemaa, and T. A. Alitouche, "Evaluation Measures for Models Assessment Over Imbalanced Data Sets," *Journal of Information Engineering and Applications*, vol. 3, no. 10, pp. 27–38, 2013, https://www.iiste.org/Journals/index.php/JIEA/article/view/7633.

[74] T. Saito and M. Rehmsmeier, "The precision-recall plot is more informative than the ROC plot when evaluating binary classifiers on imbalanced datasets," *PLoS One*, vol. 10, no. 3, p. e0118432, 2015, https://doi.org/10.1371/journal.pone.0118432.

[75] H. He and E. A. Garcia, "Learning from Imbalanced Data," *IEEE Transactions on Knowledge and Data Engineering*, vol. 21, no. 9, pp. 1263-1284, 2009, https://doi.org/10.1109/TKDE.2008.239.

[76] C. J. V. Rijsbergen, "Information Retrieval," *Butterworth-Heinemann*, 1979, https://books.google.co.id/books/about/Information_Retrieval.html?id=t-pTAAAAMAAJ&redir_esc=y.